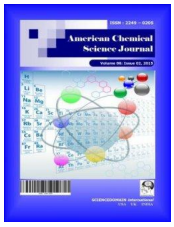

American Chemical Science Journal
7(4): 201-212, 2015, Article no.ACSj.2015.075
ISSN: 2249-0205

SCIENCEDOMAIN *international*
www.sciencedomain.org

Synthesis, Characterization and Photo Catalytic Application of TiO_2 Co-doped with Pt^{+4}, Au^{+4} and S^{-2}

Dina A. Ali[1], Hussain I. Abdulah[1] and Ramzi R. Alani[1*]

[1]Department of Chemistry, College of Science, Al-Mustansiriyah University, Baghdad, Iraq.

Authors' contributions

This work was carried out in collaboration between all authors. All authors read and approved the final manuscript.

Article Information

DOI: 10.9734/ACSj/2015/17082
Editor(s):
(1) Georgiy B. Shul'pin, Semenov Institute of Chemical Physics, Russian Academy of Sciences, Moscow, Russia.
Reviewers:
(1) Kasem K. Kasem, School of Sciences, Indiana University Kokomo, USA.
(2) Anonymous, Technical University of Cluj Napoca, Romania.
(3) Anonymous, Ege University Solar Energy Institute, Turkey.
Complete Peer review History: http://www.sciencedomain.org/review-history.php?iid=1048&id=16&aid=9244

Original Research Article

Received 25th February 2015
Accepted 21st April 2015
Published 14th May 2015

ABSTRACT

TiO_2 singly doped and Co-doped nanoparticles with Pt^{+4}, Au^{+4}, and S^{-2} ions were prepared by modified Sol-Gel method. These samples characterized by Uv-visible adsorption spectroscopy and showed red-shift in absorption band of TiO_2, XRD. showed clear anatase for all modified samples except the Au- TiO_2. AFM and SEM were used to study the morphology of the samples. The photocatalytic degradation of Para-Nitrophenol (P-NP) under visible irradiation was examined for the doped and Co-doped samples. The results shown degradation rates for singly doped in the order of: Au-TiO_2 > Au,Pt- TiO_2> Pt-TiO_2 > Au,S-TiO_2 > Pt,S-TiO_2> S-TiO_2 > undoped TiO_2 sample.

Keywords: Titanium dioxide; nanoparticles; co-doped; sol-gel method; P-Np photo degradation.

1. INTRODUCTION

Titanium dioxide (TiO_2) remains the most promising catalyst because of its high efficiency, low cost, chemical inertness, and photo stability. in spite of its wide band gap (3.2 e.v),that irradiate by using ultraviolet light for photo catalytic activation and This light accounts for only a small fraction (8%) of the sun's energy while the visible light accounts for (45%). Thus, one of the goals for improvement of the performance of TiO_2 is to increase their optical activity by shifting the onset of the response from the UV to the visible region [1,2]. Doping of TiO_2

**Corresponding author: E-mail: ramziealani@yahoo.com;*

has been an important approach in band gap engineering to change the optical properties of TiO_2. The main objective of doping is to decrease of the band gap or introduction of intra-band gap states, which can make the semiconductor able to absorb more visible light and enhanced the efficiency of its photo catalytic [3]. Many resent studies were interested in the modified of TiO_2 by doping it with metals or non metals ion to enhanced the photo activity TiO_2 [4-9]. Recent emphasis has been placed on co-doped systems, which involving combinations of cations and anions to enhancement the photo-catalytic behavior of TiO_2 [10,11]. It is highly anticipated that doping TiO_2 co-doped with two different ions would result in the development of highly efficient visible active photo catalysts [12].

To the best of our knowledge, no reports are published on TiO_2 photo catalyst co- doped with Au^{+3}, Pt^{+4}, S^{-2}. Here, TiO_2 was prepared singly doped and co-doped nanoparticles by Acid modified Sol-Gel method that can avoid the agglomeration and growth of large particles upon calcination at high temperature. The crystalline state, band gap and surface morphology of TiO_2 nanoparticles singly and co-doped samples were investigated by X-ray Diffraction (XRD), Uv-Visible spectroscopy scanning electron microscope (SEM), and atomic force microscope (AFM).The photo catalysis efficiency for photo degradation of organic pollutants, Para-Nitrophenol (P-Np), under visible light irradiation was calculated for un-doped, singly doped, and co-doped TiO_2.

2. MATERIALS AND METHODS

2.1 Materials

All reagents were used as supplied without more purification. Titanium tetrachloride (98% fluka), Adipic acid (99% Fluka), Ethanol absolute (99% Merck), Triethyl amine (98% BDH) and Silver nitrate (Sigma Aldrich), HAuCl4.XH2O(99%AlfaAesar), H2(PtCl6).6H2O (99.99% Fluka), (NH4)2SO4(BDH), Para-nitrophenol (P-Np) (BDH).

2.2 Experimental Methods

2.2.1 Preparation of $TiCl_4$ solution (SOL 1)

(0.02 mol, 3.78 g) of TiCl4 was added dropwise to (15 ml) ethanol in an ice water bath with vigorous stirring. During the addition white fume, presumably HCl, were released, A light yellow solution was obtained (Sol.1). (0.02 mol, 2.92 g.) of adipic acid was added to 20 ml of absolute ethanol with stirring then added slowly to(Sol.1) with stirring in 30 mim. A certain amount of each dopant precursor Table 1 added to 36 ml of distilled water with vigorous stirring for 1hr. at room temperature.

A gray solution was formed with continuous stirring. The solution heated at 85°C in a water bath with shaking for (4hr.) it became clear solution, then tri ethyl amine was added dropwise to the solution until the pH value reached about (8), during the addition of tri ethyl amine a white color precipitate was formed . The solution aged for 20 hr. at room temperature. The hydrous TiO2 powders washed with distilled water until all chloride were completely removed, until there was no white sediment with negative silver nitrate (0.1 M) test. The powder was obtained from the colloidal Solutions by decantation of excess water and left to dry in air at 85°C for 12hrs. The white powder was grounded to fine powder and calcined in air at temperatures ranging from 500-900°C for two hours by increasing temperature gradually.

2.2.2 Photo catalytic studies

Double jacket photo reactor cell (100 ml) with quartz window supplied by cold water circulated throughout jacket that connects to a cooling system (15°C). The Halogen lamp (150 w) that used for visible – light was placed about 15cm from the quartz window. Magnetic stirrer was used to facilitate continuous stirring of the suspension TiO2 modified sample was added to 100 ml of P-NP (10 ppm). The pH of the solution was adjusted by using HCl and NaOH solutions. The suspension was allowed to stir in the dark for 30 min. to obtain adsorption –desorption equilibrium alimented any error caused by initial adsorption. Initially 5ml aliquot was then removed. The suspension (under continuous stirring and air bubbles) was then irradiated by light. Aliquots (5 ml) were removed every 20 min. of irradiation. Collected samples were immediately centrifuged at 5000 rpm for 6min. The supernatant was decanted, then the solution was subjected to spectroscopic absorption measurement using U.v-visible spectro-photometer.

2.3 Characterization Techniques

2.3.1 X-ray diffraction (XRD)

XRD (SHIMADZU 7000, Japan, Cu Target, Ni Filter, λ=1.54Aº) were used to determine the

crystalline phase of all samples. The diffraction angle range 2θ (20-80º), the (101) peak of anatase (2θ =25.28º) and (110) peak (2θ =27.42º) of rutile were used for analysis. The phase content were determined from the ratio of peak heights in the XRD data using Spurr and Meyers equation [13].

Atomic force Microscopy (AFM) and scanning electronic microscopy (SEM): (AFM) Advanced angstrom (AA3000) Model made in USA and (SEM) Model FEI Quanta 200 Netherlands/2003 (SEM) were used to study the morphology of the prepared TiO2 samples that calcinated at 500°C.

2.3.2 Uv-visible Spectroscopy

The Uv-visible experiments were carried out on a (CARY 100 Conc.) spectrophotometer was used to record the absorbed wave length for the samples stable suspensions that prepared depending on Ping W. et.al method [14], as described below:

The samples that dried at 85°C calcined at 200°C for 2 hr. A mixture of water (5 mL.) and ethanol (5 mL) was added to the sample. The suspension was stirred for 1 hr. and treated in an ultrasonic bath for 1hr. The obtained suspensions can keep stable for 2days.

The energy gap can be calculated by using the plank equation: ($Eg = \frac{hC}{\lambda}$), Where: Eg= Band gap (Joules), h: Planck constant (6.626×10-34), λ=Cut off wave length nm (×10-9), C=speed of light =3.0×108 meter/s. The Eg will calculate in (ev)(lev=1.6×10-19Joules). The U.v-visible spectroscopy also used to record the absorption spectra of the organic pollutant P-NP at (λmax = 313 nm.).

3. RESULTS AND DISCUSSION

3.1 XRD Characterization

Fig. 1 show the XRD patterns of the TiO2 samples that singly doped with 1% mol ratio of ions (Au-TiO2), (Pt-TiO2) and (S-TiO2) samples that calciened at 500°C for 2 hr. The X.R.D patterns were consistent with the standard crystal structure of TiO2 there is no diffraction peaks associated with any of doped ions this should be ascribed to the low amount of dopants that being below the detection limit and also this indicates that specific dopant could be considered to be fully incorporation in to TiO2 lattice.

The peaks in XRD patterns of (Pt-TiO_2) and (S-TiO_2) samples can be designated to the anatase phase, the base lines indicating that they were all well crystallized while the X.R.D of (Au-TiO_2) sample Fig. 1-A shows anatase phase with small ratio of rutile phase (85/15, anatase/rutile) and the peaks were broad relative to other dopants, these observation suggest that the lattice structure of TiO_2 is locally distorted by incorporation of dopant because Au^{+3} ion has an ionic radii (0.85Å) [15] larger than the ionic radii of Ti^{+4} (0.74 Å). From this result we can believe that the Au^{+3} lowered the temperature of the anatase to rutile transformation while the Pt^{+4} ion has an ionic radii (0.76 Å) similar to Ti^{+4} So it is possibly substituted into Ti^{+4} sites of TiO_2 lattice.

Fig. 2 shows the XRD patterns of 1% mol ratio Co-doping TiO_2 samples. (Pt, S-TiO_2) and (Au, S-$TiO_{2)}$ show pure anatase phase while the sample (Pt, Au-TiO_2) patterns shows rutile phase of about 7%. The rutile was not maintained in Pt singly doped TiO_2, So this phase fraction is due to the presence of Au^{+3} ions in the samples because it is appear in Au singly doped TiO_2.

Table 1. The weight of doping ions precursors for each sample

Samples	%	Wt. of dopant precursor (g.)		
		$H_2(PtCl_6).6H2O$	$HAuCl_4.XH_2O$	$(NH_4)_2SO_4$
Pt-TiO_2	1%	0.0424	---------	--------
Au-TiO_2	1%	---------	0.0275	--------
S-TiO_2	1%	---------	---------	0.065
Pt,Au-TiO_2	1%	0.0212	0.01375	---------
Pt,Au-TiO_2	2%	0.0424	0.0275	---------
Pt,S-TiO_2	1%	0.0212	----------	0.0325
Pt,S-TiO_2	2%	0.0424	----------	0.065
Au,S-TiO_2	2%	----------	0.01375	0.065

3.2 Morphology of Modified TiO_2

The SEM images of undoped TiO_2 and singly doped TiO_2 samples shown in Fig. 3 and the AFM granularity commutation chart of undoped TiO_2 and singly doped TiO_2 samples shown in Fig. 4, all samples calciened at 500°C. The Pt-TiO_2 sample Fig. 3-B seems to be more crystalline shape compared to that of undoped TiO_2 (4-A) sample fig. 3-A and the average diameter of the particles obtained from AFM chart Fig. 4-B, is equal to (70 nm) similar to that obtained for undoped sample this show no significant change occur when the Ti^{+4} ions replaced by Pt^{+4} and this is may be due to the similarty of their ionic radii which is equal to(0.74 Å) for Ti^{+4} and equal to (0.76 Å) for Pt^{+4} [15]. So the Pt^{+4} ions are most likely to be substituted directly in Ti^{+4} sites and it can touch the surrounding oxygen atoms without distortion.

The (SEM) image of Au-doped TiO_2 sample Fig. 3-C shows that a large agglomeration and large crystals appers compared with undoped TiO_2 sample. The average diameter that obtained from (AFM) Fig. 4-C, is equal to 79.7nm which is larger than that of undoped TiO_2 and Pt-doped TiO_2 samples. This can be explained by formation of rutile phase in the sample or because of the large ionic radii of Au^{+3} ion (0.85 Å)[15] compared with Ti^{+4} that lead to little distortion in the TiO_2 lattice and because of its large ionic radii it seems to be located in interstitial position in the lattice rather than replacing the Ti^{+4} ion. The (SEM) images of S-doped TiO_2 sample that calciened at 500ºC Fig. 3-D shows a large agglomeration and give larger particle size (103.3nm) Fig. 4-D compared with the undoped one and the other doping samples. This large value may be due to larger ionic radii of S^{-2} (1.8 Å) [15] compared with O^{-2} ionic radii (1.3 Å) this may cause distortion in the lattice of TiO_2 when O^{-2} ions replaced by S^{-2} ions.

The (SEM) images of 1% mol ratio co-doped TiO_2 samples shown in Fig. 5 and the AFM granularity commutation chart of 1% mol ratio Co-doped TiO_2 samples shown in Fig. 6, all samples calciened at 500ºC. The (Au,Pt-TiO_2) sample Fig. 5-A shows smooth and homogeneous surface compared with Au and Pt singly doped TiO_2 and the average diameter of the particle's obtained from the (AFM) Fig. 6-A is equal to 86 nm for 1% Au,Pt-TiO_2 sample and 89nm for the 2% Au, Pt-TiO_2 sample Fig. 6-B, we can see some particles below 50 nm and another higher than 120 nm. that can be explained by the effect of the formation of rutile phase at low temperature in the sample and the effect of distortion of the crystal that result from the different between the ionic radii of Ti^{+4} and Au^{+3}. When the molar ratio of the doped ions increase there is no particles below 70 nm and that mean more distortion in the crystal by Au^{+3} ions.

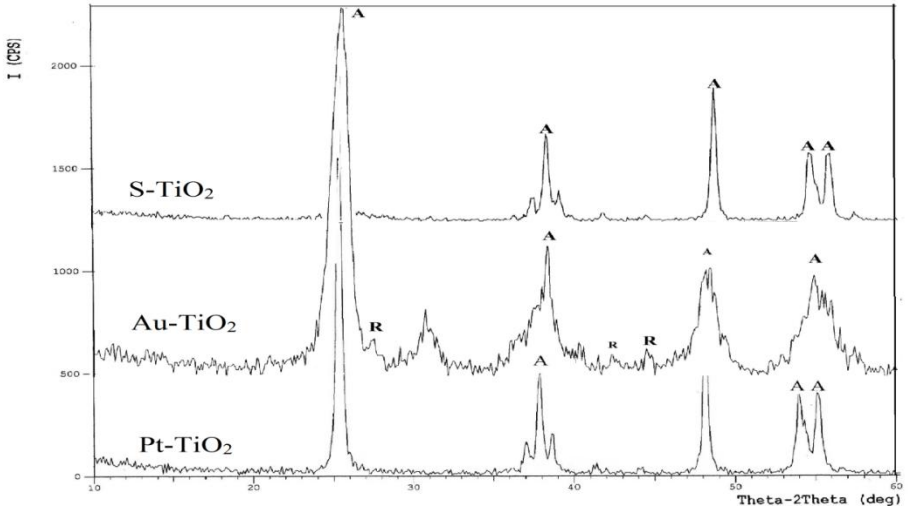

Fig. 1. XRD patterns of doped samples (A: Anatase, R: Rutile)

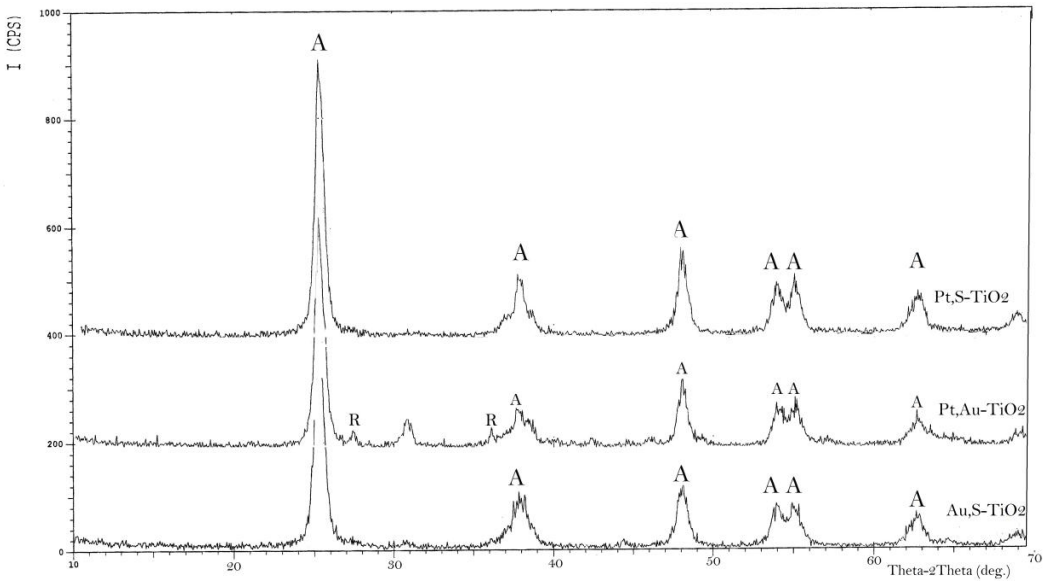

Fig. 2. The XRD patterns of Co-doped samples (A: Anatase, R: Rutile)

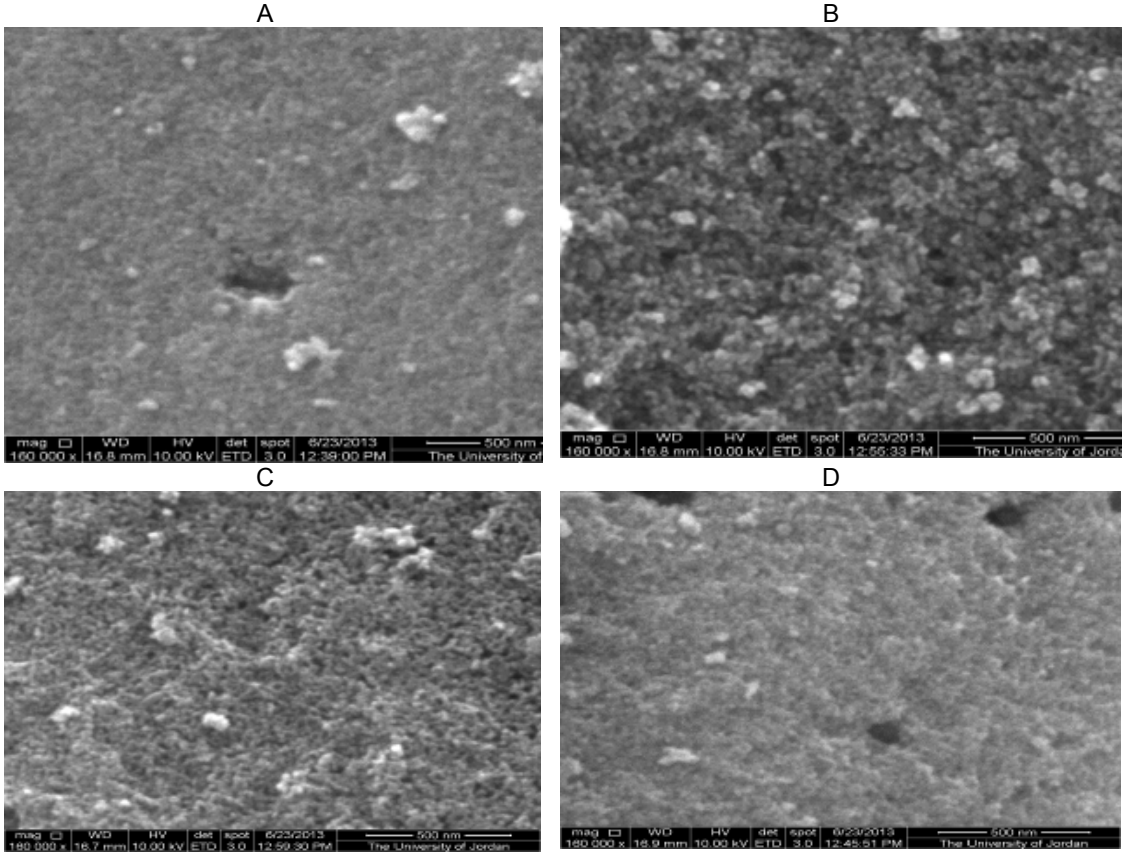

Fig. 3. The SEM image of A: undoped TiO_2, B: Pt- TiO_2, C:Au-TiO_2 ,C: S-TiO_2

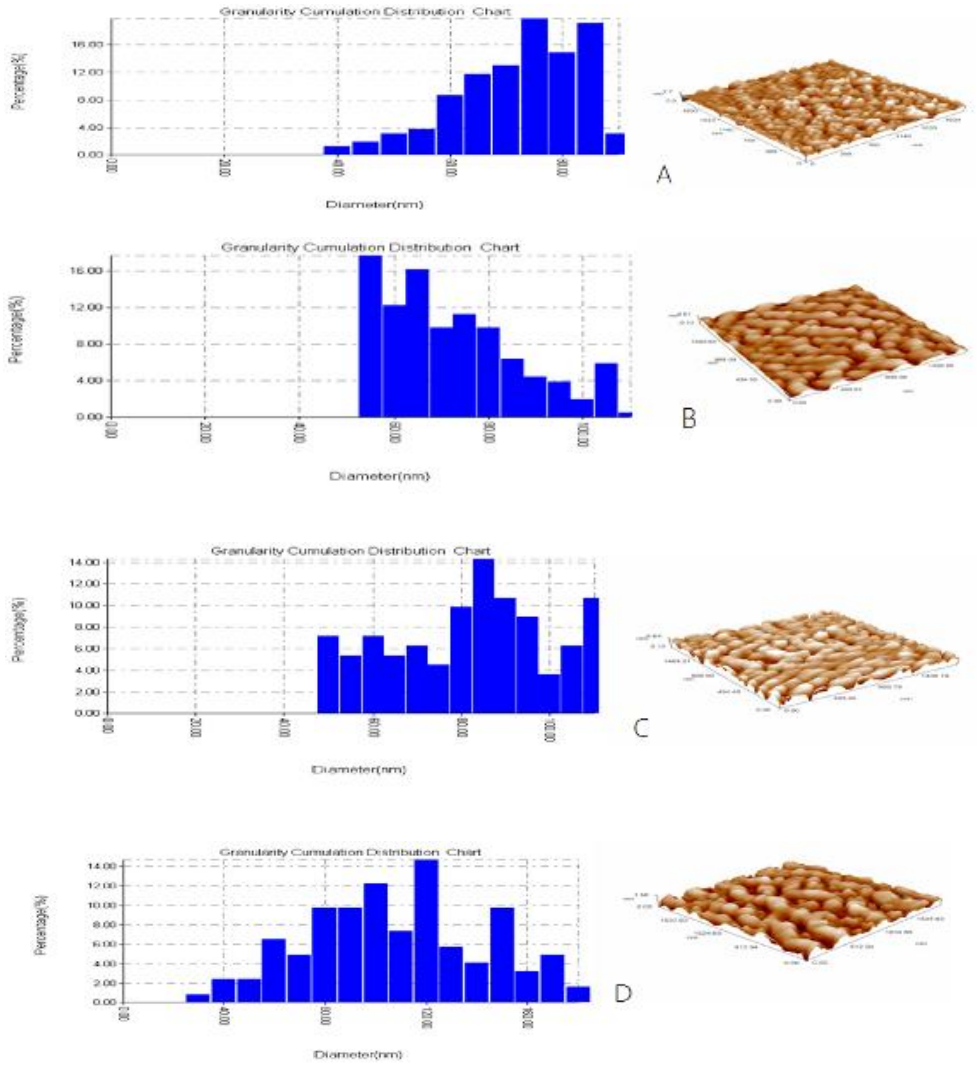

Fig. 4. The AFM granularity accumulation distribution chart A: undoped TiO_2, B: Pt- TiO_2, C:Au-TiO_2 ,D: S-TiO_2

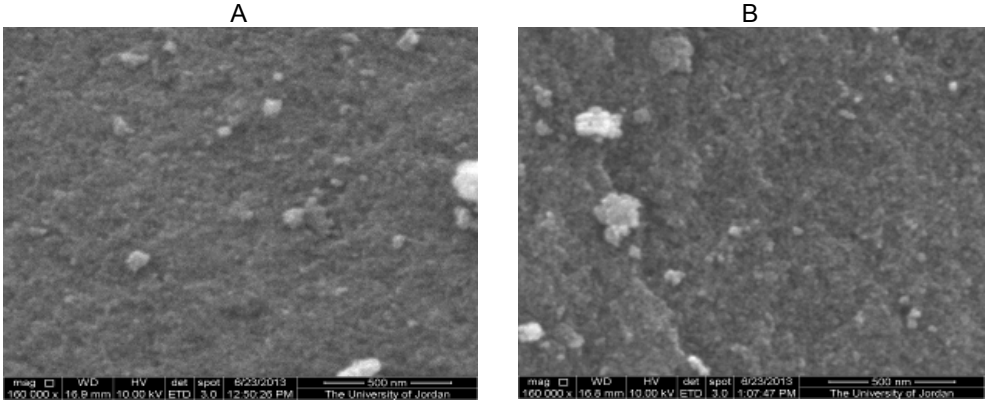

Fig. 5. The (SEM) image of 1% A: Au, Pt- TiO_2, B: Pt,S-TiO_2

The (SEM) image of (1% Pt, S-TiO_2) sample Fig. 5-B shows smooth surface with little clusters. Fig. 7 shows the (AFM) image and the average diameter of (Pt, S-TiO_2) which is equal to (83.3 nm) for the (1% Pt, S-TiO_2) sample. This value is lower than that of S^{-2} singly doped TiO_2 and higher than that of Pt^{+4} singly doped TiO_2, this is due to the decrease of the S^{-2} ions which has ionic radii higher than O^{-2} in the TiO_2 lattice which may be distorted the lattice structure .This can be improved when the amount of S^{-2} increased in the sample (2% Pt, S-TiO_2) the particle size increased too and become (90.2 nm) Fig. 7-B because more S^{-2} inter the lattice.

The images and the granularity accumulation distribution chart that obtained from (AFM) analysis for S^{-2} and Au^{+3} Co-doped TiO_2 Fig. 8 shows large crystals agglomeration with rough surface, The average diameter of particles equal to (88.3 nm) for (1% Au,S-TiO_2) sample Fig. 8-A, some large particles with diameter higher than 100 nm and another below 50 nm can be seen. This value higher than that of Au-TiO_2 sample because of the presence of S^{-2} ions as discussed above. The average diameter value increased to (97.4nm) for (2% Au, S-TiO_2) sample Fig. 8-B because of the presence of more S^{-2} ions.

From these results we can accepted that the presence of S^{-2} ion increase the particle size when co doped with another ion.

3.2.1 U.v- visible absorption spectroscopic study

Fig. 9 shows the Uv-visible absorption spectra of colloidal 1% mol ratio Co-dopedTiO2 samples as well as the undoped TiO2 sample which exhibits a sharp absorption edge at about 370 nm corresponding to the band – gap energy of 3.34ev. This value is similar to that reported value of anatase [16].

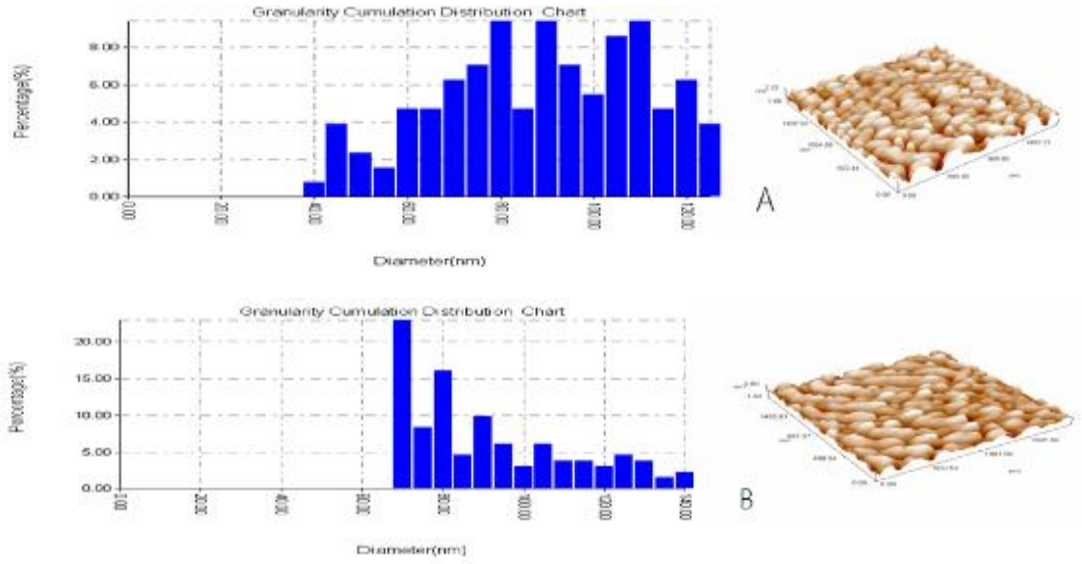

Fig. 6. The (AFM) images and the granularity cumulation distribution chart of (A) 1% Au, Pt-TiO_2 and (B) 2% Au,Pt-TiO_2

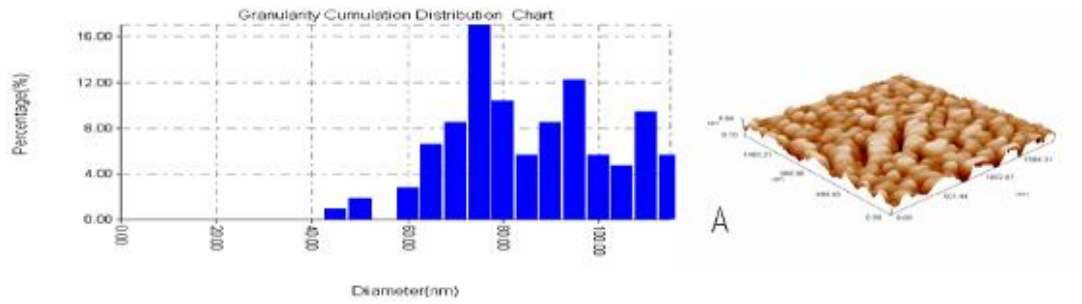

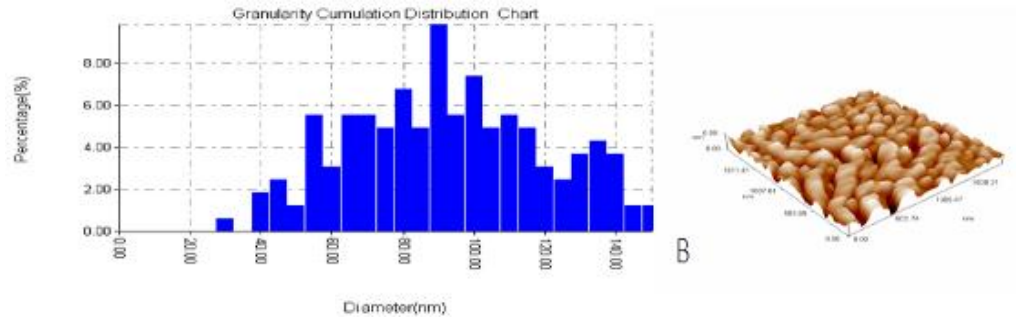

Fig. 7. The (AFM) images and the granularity accumulation distribution chart of (A) 1% Pt,S - TiO_2 and (B) 2% Pt,S-TiO_2

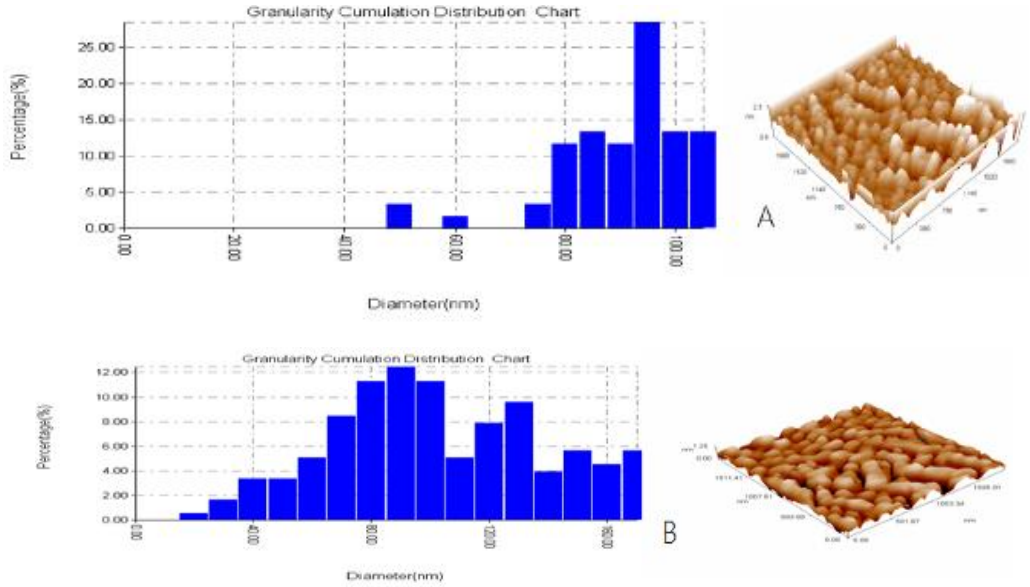

Fig. 8. The (AFM) images and the granularity accumulation distribution chart of (A) 1% Au, S-TiO_2 and (B) 2% Au,S-TiO_2

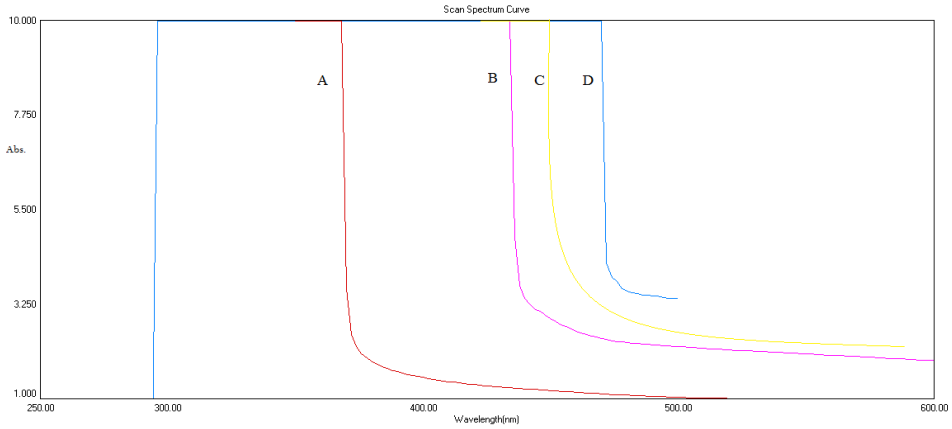

Fig. 9. The Uv- visible absorption spectra of double doped TiO2: (A): undopdTiO2 (B); Au, S-TiO2; (C): Au, Pt-TiO2; (D): Pt,S-TiO2

From the wave length absorbed by each sample of the energy gap of doped and Co-doped TiO2 can be estimated by using the equation of energy that described in the experimental. Table 2 shows the wave length and the calculated band-gap energy of all samples.

Fig. 9 shows red shift for all co-doped samples compared with undoped sample the case of Au, Pt-TiO2 sample showed a strong absorption for light at 455 nm. The red shift of absorption edge should be attributed to the presence of Au+3 and Pt+4. They cause electron transition from the valance band (VB)(O2p) to the t2g level of metal 3d orbital because this orbital located at the bottom of the conduction band of TiO2. The presence of energy level below the conduction band and above the valance band may influence the photo activity of TiO2 and thus, the dopant metal can act as electron or hole capture [17] when TiO2 doped with these two metals (Au,Pt-TiO2) the same effect of their singly doped occur.

Table 2. The band – gap energy (ev) of doped and Co-doped samples

Sample	Wave length (nm)	band energy (ev)
undopedTiO2	370	3.34
Pt,Au-TiO2	455	2.79
Pt,S-TiO2	470	2.63
Au,S-TiO2	438	2.82

In the case of (Au, S-TiO2) and (Pt, S-TiO2) samples. the result show red shift to longer wave length because of the effect of of Pt+4 and Au+3 metal ions and also the substitution of O-2 by S-2 was found to cause a significant shift in the absorption edge to lower energy by narrowing the band gap due to the mixing of the S (3P)states with the valance band [18] when this anion (S-2) doped with the other metals like (Pt+4,Au+3) the result of energy similar to that of S-2 singly doped.

3.2.2 1- Photo catalytic study

The photo degradation of P–NP in aqueous solution catalyzed by doped and co-doped TiO2 samples and compared with undoped TiO2 sample, under visible light irradiation (λ>400nm) for 100 minutes. The optimized conditions of both pH and catalyst loading of the samples were examined using the undoped sample and the results showed optimum PH at (4.5) and the optimum catalyst load (1 g/L). The Langmuir-hinshelwood (L-H) model, it has been widely used for catalytic reaction in gas-phase and liquid phase photocatalysis [19] when the concentration of water and oxygen remain constant. The kinetic rate is simplified to an pseudo-first order kinetic model:

$$Ln\frac{\mathrm{Co}}{c} = kKt = K\,\mathrm{t} \quad (1)$$

Where, C_O: Initial Concentration of the pollutant C: Concentration of the pollutant (mol/dm3), t: irradiation time (min, k: reaction rate constant (min-1), K: Langmuir constant (L/mol). The first order model was applied for all photo catalyst experiments to analyze the data. Fig. 10 shows the first order kinetic model of photo catalytic degradation of P-NP using singly doped TiO2 as well as undoped TiO2. Fig. 11 shows the first order kinetic model of photo catalytic degradation of P-NP using 1% and 2% mol ratios Co-doped samples.

The photocatalytic efficiency (_E%) is defined as Eq.(2).

$$E\% = \frac{\mathrm{Co}-\mathrm{C}}{\mathrm{C}} \times 100 \quad (2)$$

Table 3 shows the rate constant values (KP-NP) estimated from figures and also shows the photocatalytic efficiency (_E%).

The rates of degradation of P-NP were in order: Undoped TiO2 <S-TiO2-< Pt,S-TiO2< Pt,S-TiO2 < Au,S-TiO2 < Pt-TiO2<Au,Pt- TiO2 < Au-TiO2 from these results .we can see that the un doped sample has no significant effect on the degradation of P-NP due to the pure anatase phase with its wide band gap (3.2 ev), which requires ultraviolet irradiation while the TiO2-Au sample gives the higher rate constant value (KP-NP) and removal ratio (60%) better than the undoped TiO2 and the other doped-TiO2 samples after 100min of irradiation . The color of the sample is purple and it is able to absorbed visible light, this sample has a lower band gab energy value (2.69 ev) than the other doped samples. The Au can creates low-energy states within TiO2 that trap photogenerated charge carriers [20] and this will enhanced the ability to absorbed visible - light , the Pt- TiO2 sample has a rate constant value lower then that doped with Au and higher than S. Its band gap energy (2.8 ev) is higher than Au-TiO2 and lower than the sample S-TiO2. The two metal ions, Au+3,Pt+4 enhanced photo degradation under visible-light in compared to undoped sample, because both have energy level below the conduction band of TiO2 and can be rapidly trapped the excitation electrons before they falling in the halls again

[17] in addition to the presence of small ratio of rutile phase in the Au-TiO2 sample which can improve the photo reaction by the interaction of of anatase/rutile phases which result in migration of halls accumulate in rutile while electrons in anatase [21].

The data of the rate constant for the Co-doped samples showed that the 2% Co-doping ratio for each sample showed higher (K,P-NP) than that of the 1% samples. This increase of (K,P-NP)) may be because of increase in the metal and non-metal mol ratio in the samples this will give more chance to capture the electrons and enhanced the visible light absorption. The Au, Pt-TiO2 sample in dopings ratio 1% and 2% have KP-NP value lower than the Au - TiO2 and higher than Pt- TiO2 this may be due to its higher band gap energy (2.69 ev) which is similar that of Au-TiO2 (2.69 ev) and lower than that for Pt+4 (2.8 ev). So the effect of Pt+3 lowered the activity of Au, Pt- TiO2 but this sample still higher activity than the other Co-doping samples. The Au,S-TiO2 and Pt,S-TiO2 samples have the lowest (K,P-NP)) value because the presence of S-2 which has lower effect than the other dopants on the band gap energy.

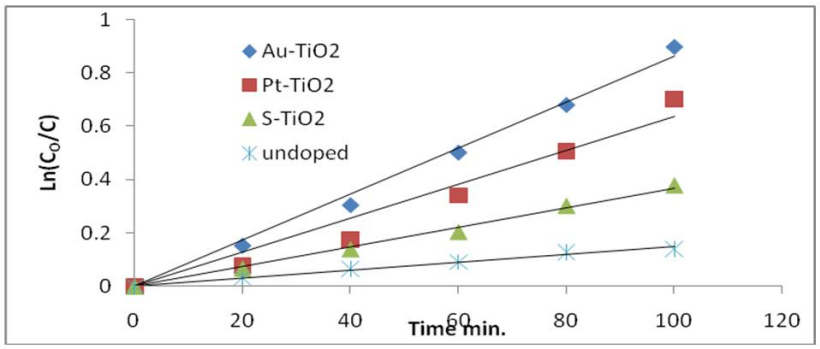

Fig. 10. The first order kinetic model of photo catalytic degradation of P-NP by singly doped TiO2

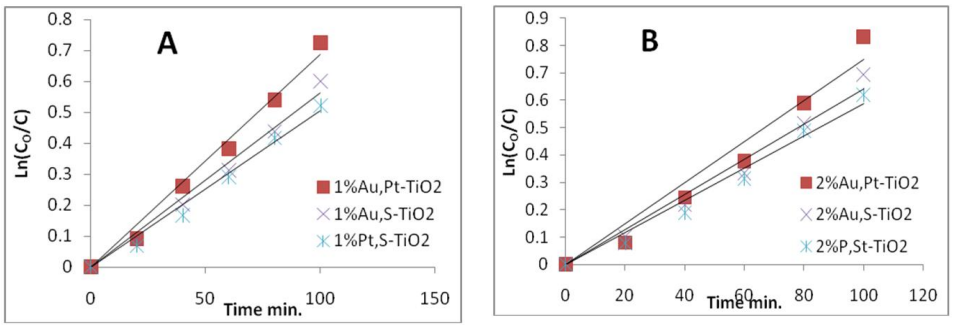

Fig. 11. The first order kinetic model of photo catalytic degradation of P-NPA: 1% and B: 2% mol ratios Co-doped samples

Table 3. The rate constant (K_{P-NP}) of the samples and the photocatalytic efficiency (_E%)

Sample	(K_{P-NP}) of 1% doping×10^{-2}	E%	(K_{P-NP}) of 2% Co- doping ×10^{-2}	E%
TiO2	0.15	13	-	-
Au-TiO2	0.86	60	-	-
Pt-TiO2	0.64	51	-	-
S-TiO2	0.42	32	-	-
Au,Pt-TiO2	0.69	52	0.75	57
Au,S-TiO2	0.56	45	0.64	50
Pt,S-TiO2	0.5	41	0.59	46

4. CONCLUSION

From the above results we conclude that the doping and Co-doping TiO2 samples with Au+3 Pt+4 and S-2 resulting a little increase in the particle size compared with undoped sample but they improved its optical activity in the visible light region by narrowing the band gap of TiO2. Most of the samples show retention of anatase phase at 500 0C except Au - TiO2 and Au, Pt-TiO2 samples show presence of small ratio of rutile and give the best photo degradation results because of the interaction of anatase/rutile phases which result in migration of halls accumulate in rutile while electrons in anatase.

COMPETING INTERESTS

Authors have declared that no competing interests exist.

REFERENCES

1. Wilcoxona JP. Photocatalysis using semiconductor nanoclusters. Advanced Catalytic Materials, MRS Boston, MA; 1998.
2. Young-Seak L, Sang J, Venkateswaran P, Jeen-Seok J, Hyuk K, Jong-Gyu K. Anion co-doped Titania for solar photocatalytic degradation of dyes. 2008;9(2):131-136.
3. 61-Carp O, Huisman CL, Reller A. Photoinduced reactivity of titanium dioxide. Prog in Solid State Chem. 2004;32:33–117.
4. Choi W, Termin A, Hoffmann MR. The role of metal ion dopants in quantum-sized TiO2: Correlation between photoreactivity and charge carrier recombination dynamics. J. Phys .Chem. 1994;98:13669.
5. Zhu J, Zheng W, He B, Zhang J, Anpo M. Characterization of Fe- TiO2 photocatalysts synthesized by hydrothermal method and their photocatalytic reactivity for degradation of XRG dye diluted in water. J Mol. Catal. A. 2004;216:35-43.
6. Fan D, Sen G, Haiqiang W, Xiaofang L, Zhongbiao W. Enhancement of the visible light photocatalytic activity of C-Doped TiO2 nanomaterials prepared by a green synthetic approach. J. Phys. Chem. C. 2011;115:13285–13292.
7. Wu JC-S, Chen CH. A visible-light response vanadium doped titania nanocatalyst by sol-gel method. J Photochem. Photobiol. A. 2004;163:509-515.
8. Zhiqiang Z, Xianyou Z, Ze W, Limin D. Mechanochemical preparation of sulfur-doped nanosized TiO2 and its photocatalytic activity under visible light. Chinese Science Bulletin. 2005;50(23): 2691-2695.
9. Rahulan KM, Padmanathan N, Balamurugan S, Philip R, Charles C. Synthesis and optical limiting studies on Au-doped TiO2 nanoparticles. Advances in Natural Sciences: Nanoscience and Nanotechnology. 2011;2:025012.
10. Sathish M, Viswanath RP, Gopinath CS. N, S-Co-doped TiO2. nanophotocatalyst: synthesis, electronic structure and photocatalysis. J. Nanoscience and Nanotechnology. 2009;9:423-432.
11. Uddin MN, Shibly SUA, Ovali R, Gulseren O, Bengu E. An experimental and first-principles study of the effect of B/N doping in TiO2 thin films for visible light photo-catalysis. Journal of Photochemistry and Photobiology A: Chemistry. 2013;254:25–34.
12. Silija P, Yaakob Z, Suraja V, Binitha NN, Akmal ZS. Review article: An enthusiastic glance in to the visible responsive photocatalysts for energy production and pollutant removal, with special emphasis on titania. International Journal of Photoenergy. Article ID 503839, 2012;19.
13. Spurr RA, Myers H. Quantitative analysis of anatase-rutile mixtures with an X-Ray Diffractometer. Anal. Chem. 1957;29(5): 760.
14. Ping Wang, Dejun Wang, Haiyan Li, Tengfeng Xie, Hongzhe Wang, Zuliang Du. A facile solution-phase synthesis of high quality water-soluble anatase TiO2 nanocrystals. Journal of Colloid and Interface Science. 2007;314:337–340.
15. Shannon RD. Revised effective ionic radii and systematic studies of interatomic distances in halides and chalcogenides. Acta Cryst. A. 1976;32:751-767.
16. Buha J. Solar absorption and microstructure of C-doped and H co-doped TiO2 thin films. J. Phys. D, Appl. Phys. 2012;45:385305.
17. Kumaresan L, Palanisamy B, Palanichamy M, Murugesan V. The syntheses, characterizations, and photocatalytic activities of silver, platinum, and gold doped TiO2 nanoparticles, Environ. Eng. Res. 2011;16(2):81-90.

18. Umebayashi T, Yamaki T, Itoh H, Asai K. Band gap narrowing of titanium dioxide by sulfur doping. Appl. Phys. Lett. 2002;81: 454.
19. Morteza M, Masoud N, Shiva J. Photocatalytic degradation of an organic dye in some aqueous buffer solutions using nano titanium dioxide: A kinetic study. Environment Protection Engineering. 2012;38(3):45.
20. Zhu J, Zheng W, He B, Zhang J, Anpo M. Characterization of Fe- TiO2 photocatalysts synthesized by hydro-thermal method and their photocatalytic reactivity for degradation of XRG dye diluted in water. J Mol. Catal. A. 2004;216:35-43.
21. Kumar SG, Devi LG. Review on modified TiO2 photocatalysis under UV/Visible light: Selected results and related mechanisms on interfacial charge carrier transfer dynamics. J. Phys. Chem. A. 2011;115: 13211–13241.

Peer-review history:
The peer review history for this paper can be accessed here:
http://www.sciencedomain.org/review-history.php?iid=1048&id=16&aid=9244